DYNAMIC MESH MODELING AND OPTIMIZATION OF A THERMOACOUSTIC REFRIGERATOR USING RESPONSE SURFACE METHODOLOGY

by

Liu LIU[a], Zhe YANG[a], Yingwen LIU[a*], and Bo GAO[b*]

[a]Key Laboratory of Thermo-Fluid Science and Engineering of MOE,
School of Energy and Power Engineering, Xi'an Jiaotong University, Xi'an, China
[b]Technical Institute of Physics and Chemistry, Chinese Academy of Sciences, Beijing, China

Original scientific paper
https://doi.org/10.2298/TSCI170911059L

In this study, a dynamic mesh model was proposed in the light of the actual working condition of an acoustic driver. Moreover, the structural optimization of the stack to improve the performance of thermoacoustic refrigerator was presented using response surface methodology. The analysis of variance was conducted to describe the rationality of regression model and examine the statistical significance of factors. Based on the consideration of parameters interaction, the optimized values of stack parameters suggested by response surface methodology have been predicted successfully. Results showed that optimal stack parameters group could realize the optimal cooling performance. The optimal ratios of stack spacing to stack thickness and stack length to stack position were 3.59-4 and 0.77-1, respectively. This study provides a new method for CFD modeling and optimizing the thermoacoustic refrigerator, which helps to popularize its application.

Key words: *CFD, response surface methodology, cold end solid temperature, thermoacoustic refrigerator*

Introduction

Thermoacoustics is a branch of science dealing with the conversion of heat energy into sound energy and *vice versa*. With society's current focus on human impact upon the environment, renewable sources of energy, and the inability for current energy grid systems to fully fill needs for remote and developing civilizations at feasible cost, the development of the thermoacoustic device is a pursuit worth exploring. Compared with traditional refrigerators, thermoacoustic refrigerators (TAR) have advantages of no moving parts, environmental friendliness and potential high efficiency [1].

Stack added in the resonator will expand the contact region between the solid wall and the oscillatory flow, thus strengthen the thermoacoustic effect. Therefore, the structural parameters of the stack directly affect the cooling performance. A 2-D numerical simulation of TAR was carried out by Ke *et al.* [2] to identify optimized parameters of plate thickness, plate spacing and length of heat exchangers. Zink *et al.* [3] used an optimization based ap-

* Corresponding autor, e-mail: ywliu@xjtu.edu.cn; bgao@mail.ipc.ac.cn

proach in conjunction with a finite element solver to identify optimal solutions to their two--variable model. Tijani *et al.* [4] combined DeltaEC with experiments to optimize the geometry of the stack. Bassem [5] optimized the diameter of stack and its installation site experimentally. These literature previously analyses exhibited a lack of study on the interaction effects of the stack parameters. Therefore, in order to consider the interaction of stack parameters and reduce the complexity of experimental process, response surface methodology (RSM) was employed to optimize the performance of thermoacoustic systems [6, 7]. During the process of implementation, RSM can analyze the effect of independent variables, alone or in combination statistically. Desai *et al.* [8] investigated that significant of stack position and stack length for engine stack, stack position, and stack length for refrigerator stack. Hariharan *et al.* [9] optimized the parameters like plate spacing and frequency engaged in designing TAR. Their results show that geometrical variables chosen for investigation are independent.

In this paper, the dynamic mesh model is proposed according to the actual working condition of the acoustic driver. The most important parameters influencing the performance of TAR are plate spacing, plate thickness, stack length, and stack position. Next, the influences of stack parameters on the temperature at the cold end of the stack are investigated by RSM. Finally, the optimized parameters of stack are obtained to improve the cooling performance of thermoacoustic refrigerator.

Modeling for thermoacoustic refrigerator

Numerical model for thermoacoustic refrigerator

In this paper, a model of a 1/2-wavelength TAR is developed and its computational domain is shown in fig. 1. One end of the model is the acoustic driver which is used to input sound wave, and the other end is closed. In order to simplify model and save time, the CFD domain fully considered the symmetry and periodicity of oscillatory flow. The main parameters which are used in the computations are A, B, C, and D which denoted plate spacing (the distance between the centers of two plates), plate thickness, stack length, and stack position, respectively.

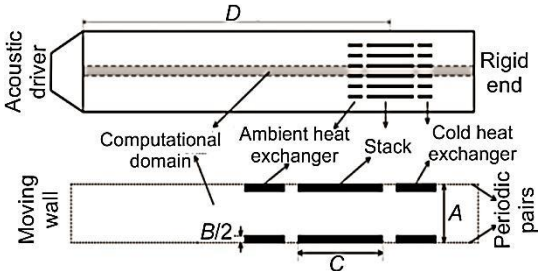

Figure 1. Schematic illustration of TAR

In FLUENT 6.3.26, the acoustic end driver is replaced by moving rigid wall. The moving wall is implemented by dynamic mesh model. Following the local ideal standing propagation, the velocity of the moving wall is governed by:

$$u_{\text{wall}} = u_a \sin(\omega t) \tag{1}$$

$$u_a = \frac{p_a}{\rho_m a} \tag{2}$$

where u_a is the amplitude of the dynamic velocity, ω – the angular frequency, p_a – the amplitude of the dynamic pressure, a – the sound speed, and ρ_m – the mean density.

The governing equations are given:

$$\frac{\partial(\rho_f)}{\partial t} + \frac{1}{r}\frac{\partial}{\partial x}(\rho_f v_x) = 0 \tag{3}$$

$$\frac{\partial}{\partial t}(\rho_f v) + \nabla(\rho_f vv) = -\nabla p + \nabla(\boldsymbol{\tau}) \tag{4}$$

$$\frac{\partial}{\partial t}(\rho_f E) + \nabla\left[v(\rho_f E + p)\right] = \nabla\left[\hat{k}\nabla T + (\boldsymbol{\tau}\cdot v)\right] \tag{5}$$

where r and x represent the radial and axial direction in the cylindrical co-ordinate, respectively, E and h are internal energy and enthalpy, respectively, ρ_f, v, p, T, τ, and k are density, velocity, pressure, temperature, stress tensor, and thermal-conductivity coefficient, respectively. Working gas is helium, assumed to be an ideal gas. The state equation is $p = \rho_f RT$ where R is the gas constant, 287 J/kgK.

In this paper, the pressure-based solver and the second-order implicit time differencing has been used. The SIMPLE algorithm and the one-order upwind spatial difference have been selected. As for time step, by contrast, a fixed time step of 1e-05 is selected. The absolute convergence criteria for mass, momentum, energy, k and ε equation are 1e-05, 1e-03, 1e-06, and 1e-03, respectively. The total length of the model is 600 mm. The mean pressure of helium is 1 MPa and the initial temperature is 300 K. The driving frequency is 860 Hz. The materials of stack and heat exchangers are steel and Cu, respectively. The initial temperature of ambient and cold heat exchanger is set at 300 K and 260 K, respectively. At the solid-gas interfaces, thermally coupled boundary conditions are imposed to calculate the heat convection between the solid stack and working gas. The stack is considered as conjugate heat transfer boundary condition:

$$T_{g,\text{wall}} = T_{s,\text{wall}} \tag{6}$$

$$k_g \frac{\partial T_g}{\partial n} = k_s^{\text{eff}} \frac{\partial T_s}{\partial n} \tag{7}$$

where n is the local co-ordinate normal to the wall, T_g – the gas temperature, T_s – the stack temperature, k_g – the gas thermal conductivity, and k_s^{eff} – the stack effective thermal conductivity.

Advantage of dynamic mesh model

To verify the accuracy of dynamic mesh model, the results are compared to the model with pressure inlet and mass-flow inlet conditions. Figure 2 presents the net mass-flow in one cycle at the entrance as pressure ratio increases. It can be seen that the net mass-flow with the dynamic mesh and mass-flow inlet conditions changes slightly around zero, which indicates the mass-flow at the entrance is conservative. However, the conservation of mass-flow with the pressure inlet condition is not well, and becomes worse as pressure ratio increases.

The mass inlet is used for the known inlet mass-flow. For the import fluctuation boundary condition, the dynamic mesh technique could be a way to solve the phenomenon of backflow at the inlet of the thermoacoustic refrigerator, and more in line with the actual situation of the speaker drive. Therefore, it is convincing that the dynamic mesh is suitable for modelling thermoacoustic refrigerator.

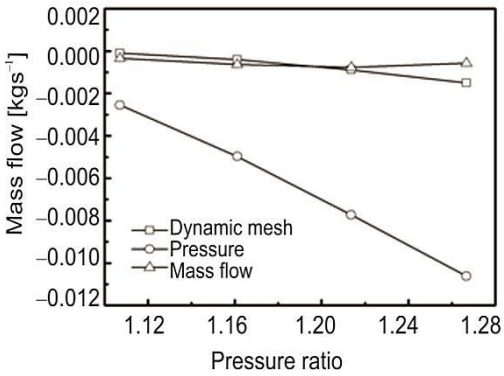

Figure 2. The variation of net mass-flow as pressure ratio increases

Results and discussion of RSM

The RSM is an assembly of statistical and mathematical method useful for developing, refining, and optimizing process. It deals with the circumstances where several input variables potentially affect the performance quality or the measure of a product or a process which are known as responses. The objective is to establish a suitable approximation of the true functional relationship between independent variables and the process responses through RSM. Generally, a second-order model utilized in RSM is given:

$$y = \beta_0 + \sum_{i=1}^{k} \beta_i x_i + \sum_{i=1}^{k-1} \sum_{j=i+1}^{k} \beta_{ij} x_i x_j + \sum_{i=1}^{k} \beta_{ii} x_i^2 + \varepsilon \tag{8}$$

where y is the corresponding response for input variables while x_i, $x_i x_j$, and x_i^2 are the square and interaction terms of parameters, respectively. The β_0, β_i, β_{ij}, and β_{ii} are the unknown regression coefficients while ε is the error. The Box-Behnken design (BBD) is selected to generate the design matrix since it needs fewer experiments when the number of factors is about 3 to 4. Four factors and three levels (–1, 0, +1) are used for construction of second-order response surface model. The influence of stack parameters on the cooling effect is investigated. The cold end solid temperature is used to evaluate the cooling effect. The ranges of stack parameters are shown in tab. 1.

Table 1. Ranges of stack parameters

Parameters	Real values of coded levels		
	–1	0	1
Plate spacing (A), [mm]	0.23	0.34	0.45
Plate thickness (B), [mm]	0.06	0.1	0.14
Stack length (C), [mm]	48	68	88
Stack position (D), [mm]	70	100	130

The ANOVA analysis

Analysis of variance (ANOVA) is carried out to observe the variance of variables and obtain the evaluation index of variance. In ANOVA, the sum of squares is used to estimate the square of deviation from the grand mean. Mean squares are estimated by dividing the sum of squares by degrees of freedom. According to the arrangement of design points in BBD, each run with different factor groups is input in CFD model to obtain the corresponding response. To reduce random error and ensure uniformity of parameters, the experiment of center point is repeated three times. The design of experimental matrix including factors and responses is shown in tab. 2. In terms of actual factors, the quadratic model in the form of a regression equation for cold end temperature is given:

$$\begin{aligned} T_{\text{cold end}} = {} & 222.82354 + 18.87259A + 328.23295B - 0.030534C + 0.33325D - \\ & -767.04545AB - 0.15909AC + 0.41667AD - 0.34375BC - 1.06250BD - \\ & - 4.41667E\text{-}003CD + 99.17355A^2 + 101.56250B^2 + 3.21875E\text{-}003C^2 + 1.111111E\text{-}004D^2 \end{aligned} \tag{9}$$

The ANOVA results of the quadratic model for cold end temperature are presented in tab. 3. From tab. 3, the F-value of 31.56 in the ANOVA table implies that the model is significant. The p-value ($Prob > F$) is an improtant factor to judge whether a term has significant effect on the response or not. For p-values less than 0.05 (*i. e.*, $\alpha = 0.05$, or 95% confi-

dence), indicating that the corresponding terms are significant statistically. In this case, A, B, C, D, AB, AD, BD, CD, A^2, and C^2 are significant terms of thermoacoustic model. Other terms AC, BC, B^2 are not significant.

Table 2. Design of experimental matrix

Run	Stack parameters				Result
	Plate spacing A, [mm]	Plate thickness B, [mm]	Stack length C, [mm]	Stack position D, [mm]	Cold end solid temperature, [K]
1	0.23	0.06	68	100	258.1
2	0.45	0.06	68	100	275.5
3	0.23	0.14	68	100	261.1
4	0.45	0.14	68	100	265.2
5	0.34	0.10	48	70	262.1
6	0.34	0.10	88	70	263.8
7	0.34	0.10	48	130	271.3
8	0.34	0.10	88	130	262.5
9	0.23	0.10	68	70	257.7
10	0.45	0.10	68	70	264.2
11	0.23	0.10	68	130	261.8
12	0.45	0.10	68	130	273.8
13	0.34	0.06	48	100	268.8
14	0.34	0.14	48	100	265.9
15	0.34	0.06	88	100	263.7
16	0.34	0.14	88	100	259.7
17	0.23	0.10	48	100	264.6
18	0.45	0.10	48	100	272.4
19	0.23	0.10	88	100	259.7
20	0.45	0.10	88	100	265.7
21	0.34	0.06	68	70	260.7
22	0.34	0.14	68	70	260.4
23	0.34	0.06	68	130	268.7
24	0.34	0.14	68	130	263.3
25	0.34	0.10	68	100	263.2
26	0.34	0.10	68	100	263.2
27	0.34	0.10	68	100	263.2

The R^2 value for cold end temperature is 0.9693, which is defined as the ratio of the explained variation to the total variation and an adjusted determination coefficient value (Adj *R*-Squared) 0.9386, which is nearer to unity and encourages the high correlation between the actual (CFD) and the predicted (RSM) values. The *Adeq Precision* measures the signal to noise ratio. A ratio greater than four is desirable. For the present study, the ratio of signal to noise was found to be 19.709. Therefore, this model can be used to navigate the design space.

The interaction terms AB and CD have lower *p*-values than the squared terms of A, B, C, D and the other interaction terms. The two interaction terms are more significant due to lower *p*-values and higher *F*-value. So, the interaction terms AB and CD are mainly discussed here.

Table 3. The ANOVA table for cold end solid temperature

Source	Sum of squares	*df*	Mean square	*F*-value	*p*-value Prob > *F*	
Model	538.66	14	38.48	31.56	< 0.0001	significant
A-plate spacing	237.63	1	237.63	194.94	< 0.0001	significant
B-plate thickness	33.67	1	33.67	27.62	0.0001	significant
C-stack length	72.52	1	72.52	59.49	< 0.0001	significant
D-stack position	88.56	1	88.56	72.65	< 0.0001	significant
AB	45.56	1	45.56	37.38	< 0.0001	significant
AC	0.49	1	0.49	0.40	0.5363	
AD	7.56	1	7.56	6.20	0.0259	significant
BC	0.30	1	0.30	0.25	0.6261	
BD	6.50	1	6.50	5.33	0.0367	significant
CD	28.09	1	28.09	23.04	0.0003	significant
A^2	9.34	1	9.34	7.66	0.0151	significant
B^2	0.17	1	0.17	0.14	0.7134	
C^2	10.75	1	10.75	8.82	0.0101	significant
D^2	0.065	1	0.065	0.053	0.8209	
Residual	17.07	14	1.22			
Lack of fit	17.07	10	1.71			
Pure error	0	4	0			
Cor total	555.73	28				
Adeq Precision = 19.709				Pred *R*-Squared = 0.8231		
R-Squared = 0.9693				Adj *R*-Squared = 0.9386		

Figure 3 presents cold end temperature values obtained from CFD and the RSM--generated model. It is observed from this figure that the deviation of cold end temperature is within ±1%. It is shown that there is a pretty good agreement between actual and predicted values. Since the points are distributed evenly on the diagonal line, which indicates that the quadratic model developed for temperature difference can be used to accurately predict the cold end temperature within the range of designing parameters.

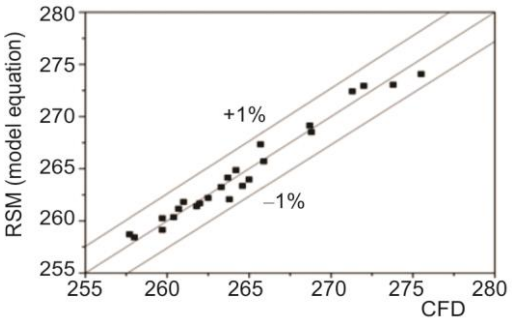

Figure 3. The CFD value *vs*. RSM value

Influence and interaction of parameters on the cold end temperature

Influence of plate spacing and plate thickness

The interaction effects of plate spacing and plate thickness on the cold end temperature are visualized through response surface plot and contour plot shown in fig. 4 when stack length and position are fixed at 61.67 mm and 70 mm. When plate thickness is small, cold end solid temperature increases with plate spacing. While plate thickness is larger, cold end solid temperature increases with plate thickness at small plate spacing, whereas it decreases with an increase in plate thickness at large plate spacing.

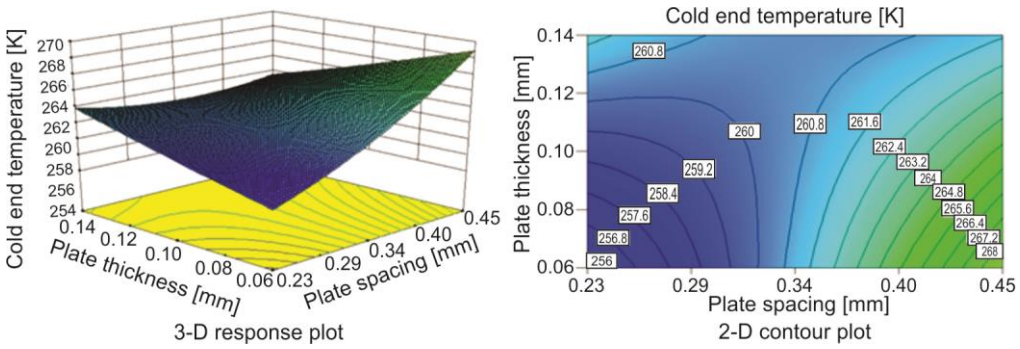

Figure 4. Interaction effect of plate spacing and plate thickness on cold end temperature

It can be concluded that the interaction effect of plate spacing and plate thickness is very complex. The thermoacoustic effect usually takes place in the boundary-layer which is approximately one penetration depth of the working fluid. Generally speaking, the spacing between plates is about 2-4 times the penetration depth [10]. If plate spacing is too large, the thermoacoustic effect occurs only in the boundary-layer, yet most working fluid can not participate in the thermoacoustic effect. And too small plate spacing will intensify the viscous loss near the plate, thus weakening the thermoacoustic effect. Therefore, there should be an optimal plate spacing value to achieve the lowest cold end solid temperature. Besides, viscous loss increases with plate thickness. However, too small plate thickness is not always good for cooling effect. Therefore, a suitable plate thickness is also important as well. In order to obtain the optimal match between plate spacing and plate thickness, the ratio of plate spacing to plate thickness is analyzed. When plate thickness is 0.06 mm, as the ratio increases from 3.8 to 7.5 with the increase in plate spacing, the minimal cold end solid temperature is achieved with the ratio of 3.8. When plate spacing is 0.23-0.24 mm and plate thickness is 0.06 mm, the cold end solid temperature achieves the lowest value (lower than 256 K). When plate thickness is 0.06-0.064 mm and plate spacing is 0.23 mm, the cold end solid temperature achieves the lowest value (lower than 256 K). Overall, it can be concluded that optimal ratio of plate spacing to plate thickness is 3.59-4.

Influence of stack length and stack position

The combined influences of stack length and stack position on cold end solid temperature are visualized through response surface plot and contour plot shown in fig. 5 when plate spacing and plate thickness are fixed at 0.23 mm and 0.06 mm. The change of cold end solid temperature as stack length and stack position is similar to that in fig. 4. Long stack means more working gas participate in thermoacoustic effect, however, the viscous loss also increases at the same time. Therefore, a suitable stack length is important for improving the cooling effect. When stack is near to the moving wall which is close to pressure antinode, the strong expansion and compression of the working gas will improve the cooling effect. Nevertheless, it should be noted that gas velocity is small near pressure antinode, which will weaken heat exchange between stack and ambient working gas. As stack move toward the pressure node, the whole process is opposite to that near pressure antinode. As a result of the two contradicting aspects, there must be an optimal stack position in which the lowest cold end solid temperature can be achieved. Similarly, when stack length is 54-70 mm and stack position is 70 mm, the cold end solid temperature achieves the lowest value (lower than 256 K). Therefore, the optimal ratio of stack length to stack position is 0.77-1.

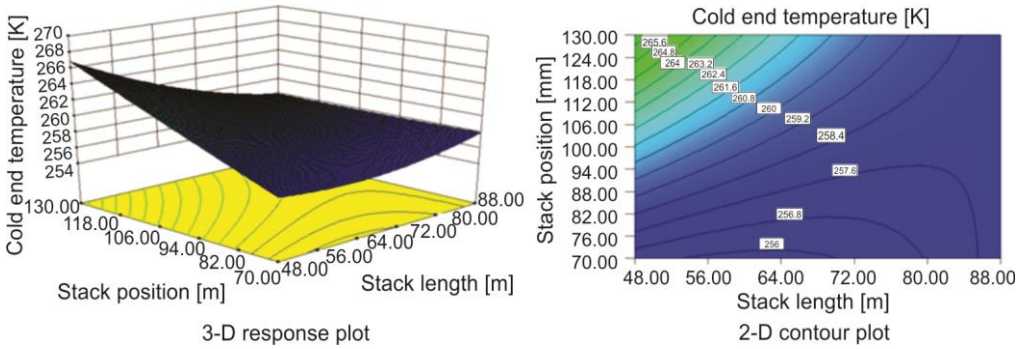

Figure 5. Interaction effect of stack length and stack position on cold end solid temperature

Conclusions

In this study, the dynamic mesh model was presented to simulate a thermoacoustic refrigerator according to the actual working characteristic of the driver. The RSM was used to investigate the influences of the parameters of the stack on the performance of a thermoacoustic refrigerator, where the interaction effects between parameters are considered. An effective mathematical model has been developed for optimization of TAR system. The impacts of plate spacing, plate thickness, stack length and stack position on the cold end solid temperature of the stack were analyzed statistically. The effectiveness of the developed RSM model was verified using ANOVA. The ANOVA analysis shows that the quadratic model generated in the RSM for the response of TAR is accurate to predict the performance of the thermoacoustic refrigerator. It was also found that all the four factors are influencing the performance of the TAR significantly, which is also confirmed by low *p*-value. Finally the parameters of the stack were optimized to obtain the lower cold end temperature. Results showed that the optimal ratio of plate spacing to plate thickness and ratio of stack length to stack position are 3.59-4 and 0.77-1, respectively.

Acknowledgment

This work is financially supported by National Key R&D Program of China (2016YFE0204200) and the National Natural Science Foundation of China (No. 51576150).

Nomenclature

A – plate spacing, [m]
B – plate thickness, [m]
C – stack length, [m]
D – stack position , [m]
x_i, x_j – variables, [–]
y – response, [–]

Greek symbols

β_0 – intercept, [–]
β_i – linear effect, [–]
β_{ii} – squared effect, [–]
β_{ij} – interaction effect, [–]
ε – error, [–]

Superscript

k – number of factors, [–]

References

[1] Zink, F., *et al*., CFD Simulation of Thermoacoustic Cooling, *International Journal of Heat and Mass Transfer*, *53* (2010), 19-20 , pp. 3940-3946
[2] Ke, H. B., *et al.*, Numerical Simulation and Parameter Optimization of Thermo-Acoustic Refrigerator Driven at Large Amplitude, *Cryogenics*, *50* (2010), 1, pp. 28-35

[3] Zink, F., *et. al.*, Geometric Optimization of a Thermoacoustic Regenerator, *International Journal of Thermal Sciences, 48* (2009), 12 , pp. 2309-2322
[4] Tijani, M. E. H., *et al*., Design of Thermoacoustic Refrigerators, *Cryogenics, 42* (2002), 1, pp. 49-57
[5] Bassem M. M., *et al*., Design and Construction of a Traveling Wave Thermoacoustic Refrigerator, *International Journal of Refrigeration, 34* (2011), 4, pp. 1125-1131
[6] Yang, P., *et al*., Prediction and Parametric Analysis of Acoustic Streaming in a Thermoacoustic Stirling Heat Engine with a Jet Pump Using Response Surface Methodology, *Applied Thermal Engineering, 103* (2016), June, pp. 1004-1013
[7] Yang, P., *et al*., Application of Response Surface Methodology and Desirability Approach to Investigate and Optimize the Jet Pump in a Thermoacoustic Stirling Heat Engine, *Applied Thermal Engineering, 127* (2017), Dec., pp. 1005-1014
[8] Desai A. B., *et al.*, Optimization of Thermoacoustic Engine Driven Thermoacoustic Refrigerator Using Response Surface Methodology, *Proceedings*, 26th IOP Conf., New Delhi, India, 2017, Vol. 171, pp.1-8
[9] Hariharan N. M., *et al*., Optimization of Thermoacoustic Prime Mover Using Response Surface Methodology, *HVAC & R Research, 18* (2012), 5, pp. 890-903
[10] Swift G. W., Garrett S. L., Thermoacoustics: A Unifying Perspective for Some Engines and Refrigerators, *J. Acoust. Soc. Am., 113* (2003), 5, pp. 2379-2381

Paper submitted: September 11, 2017
Paper revised: December 19, 2017
Paper accepted: December 22, 2017